

Localization persisting under aperiodic driving

Hongzheng Zhao,^{1,2} Florian Mintert,² Johannes Knolle,^{3,4,2} and Roderich Moessner¹

¹Max-Planck-Institut für Physik komplexer Systeme, Nöthnitzer Straße 38, 01187 Dresden, Germany

²Blackett Laboratory, Imperial College London, London SW7 2AZ, United Kingdom

³Department of Physics TQM, Technische Universität München, James-Frank-Straße 1, D-85748 Garching, Germany

⁴Munich Center for Quantum Science and Technology (MCQST), 80799 Munich, Germany

Localization may survive in periodically driven (Floquet) quantum systems, but is generally unstable for aperiodic drives. In this work, we identify a hidden conservation law originating from a chiral symmetry in a disordered spin- $\frac{1}{2}$ XX chain. This protects indefinitely long-lived localization for general—even aperiodic—drives. Therefore, rather counter-intuitively, adding further potential disorder which spoils the conservation law *delocalizes* the system, via a controllable parametrically long-lived prethermal regime. This provides a first example of persistent single-particle ‘localization without eigenstates’.

Introduction.— Closed quantum many-body systems with time-dependent (‘driven’) Hamiltonians tend to absorb energy until they reach a featureless ‘infinite temperature’ state [1–3]. This heat death can be prevented if a sufficient number of integrals of motion is present. This may occur in integrable systems [4], or via the emergent structure underpinning many-body localization [5], which is stable against periodic driving for sufficiently strong disorder [6, 7]. This even allows for novel non-equilibrium phenomena such as discrete time crystalline order [8, 9] and anomalous Floquet-Anderson insulators [10].

In recent years, the focus has shifted to aperiodic drives to control quantum systems [11–22]. This leads to new types of dynamical phenomena, e.g. non-adiabatic topological energy pumps [23–25] and prethermalization with algebraically scaling lifetimes [26, 27]. However, the absence of time translation symmetry (TTS) is generally expected to generate stronger heating effects, in particular destabilizing localization [12, 13]. Nonetheless, localization has been shown to remain robust for two-tone continuous drives [14], paving the way to stabilize non-equilibrium phases unobtainable with periodic drives, e.g., the quantum Hall effect in synthetic dimension [15–18] and discrete-time quasicrystals [12, 13, 19].

One natural question, then, is under what conditions localization can indefinitely survive generic aperiodic and even random driving profiles? Unlike multi-tone drives with few frequency components [12, 14], generic drives contain low-frequency components which normally induce delocalization. Technically (and conceptually), the analysis of generic aperiodic drives is complicated as no way is known of analysing the quantum dynamics in terms of a fixed set of eigenstates, $\{\psi_i\}$, whose time evolution is described by a simple phase accumulation rate given by their respective (quasi-)energies ϵ_i .

Here, we show that a localized steady state can emerge in a non-interacting multi-particle system subjected to a drive with a well-defined coupling operator but general time-dependence and in this sense represents single-particle localization without eigenstates.

Our model hosts disorder not as an on-site potential but instead via randomness in the exchange interactions (or hopping amplitudes for fermions) [28–30]. The disordered exchange interaction has a single-particle chiral symmetry resulting in a spectrum symmetric around zero. Unlike the single-particle localization induced by potential disorder, where all eigenstates are localized, the chiral symmetric randomness does not fully localize all eigenstates, but instead yields a diverging localization length at zero energy [31–34]. Crucially, this chiral symmetry enables us to construct drives with a hidden conservation law, and we demonstrate that the localized steady state persists indefinitely for arbitrary aperiodic drives as long as the conservation law is preserved.

A static disorder-free exchange without the chiral symmetry, or potential disorder, destroys this feature. They do so via different routes, as the latter counterintuitively combines the *addition* of disorder with *delocalization* as the symmetry is broken. This ‘competition’ gives rise, as a function of disorder strength, to a non-monotonic heating rate. The resultant ‘prethermal’ localized state can also be exceptionally long-lived upon increasing the driving frequency.

In the following, we first introduce the model with the single-particle chiral symmetry, and show that the system reduces to a collection of two-level systems. Each pair corresponds to the localized chiral symmetric excitations at opposite energies $\pm\epsilon_i$. We then construct a drive which only introduces dynamics within each two-level system. Therefore, single-particle localization always persists despite the absence

of well-defined eigenstates for generic aperiodic drives. For a multi-particle state, however, the single-particle chiral symmetry does not straightforwardly generalize. Instead, we show that it leads to an extensive number of local conserved quantities which can protect the multi-particle steady state from delocalization.

We then focus on the aperiodic Thue-Morse (TM) drive to numerically verify the existence of persistent localization via analyzing both the single-particle time evolution operator and the entanglement generation for multi-particle states. We finally show how different types of chiral symmetry-breaking perturbations lead to a long-lived prethermal regime with *non-monotonic* scalings of the prethermal lifetime.

The model and hidden conservation law.— We focus on the spin-1/2 model described by the Hamiltonian

$$H(t) = H_0 + \delta h f(t) \hat{P}, \quad (1)$$

where the nearest-neighbor exchange interaction reads $H_0 = \frac{1}{4} \sum_i J_i (\sigma_i^x \sigma_{i+1}^x + \sigma_i^y \sigma_{i+1}^y)$ with disordered coupling strength $J_i \in [J_0, J_0 + J_{max}]$. The staggered potential $\hat{P} = \sum_i (-1)^i \sigma_i^z / 2$ is modulated with the amplitude δh according to a time-dependent function $f(t)$ which will be specified later. Since $[H_0, \hat{P}] \neq 0$, the drive is not trivially equivalent to a quench. This model can be transformed into a non-interacting fermionic form (Eq. 2) via the Jordan-Wigner transformation [35]

$$H(t) = \sum_i \frac{J_i}{2} (c_i^\dagger c_{i+1} + h.c.) + \delta h f(t) \sum_i (-1)^i n_i, \quad (2)$$

with the standard fermionic operators $c_i^{(\dagger)}$ and the number operator n_i . The model has a $U(1)$ symmetry, hence, the total particle number, or the total magnetization in spin language, is conserved. As the nearest-neighbor hopping is disordered, eigenstates of H_0 are localized (or quasi-localized if the corresponding eigenenergies are close to zero [36, 37]). As shown in the following, the Hamiltonian H_0 has a hidden conservation law even in the presence of \hat{P} which can protect the system from delocalizing regardless of the driving profile $f(t)$.

This conservation law originates from a single particle chiral symmetry of the Hamiltonian H_0 . Consider a general real quadratic Hamiltonian $H_C = \sum_{ij} c_i^\dagger A_{ij} c_j$, its anti-commutator with the staggered potential $\hat{P} = \sum_i (-1)^i n_i$ reads

$$\{H_C, \hat{P}\} = \sum_{ij} [(-1)^i + (-1)^j] A_{ij} c_i^\dagger c_j + \hat{D}. \quad (3)$$

with $\hat{D} = 2 \sum_{ijk} (-1)^k A_{ij} c_i^\dagger n_k c_j$. Crucially, the matrix elements of \hat{D} can be non-zero only for multi-particle states, but

they vanish in the single-particle subspace. In addition, for the Hamiltonian H_0 considered in Eq. 1, the first contribution on the right hand side of Eq. 3 vanishes because A_{ij} is nonzero only for $j = i + 1$; in this case, however, the corresponding prefactor $(-1)^i + (-1)^j$ vanishes. The anti-commutator $\{H_0, \hat{P}\}$ thus vanishes in the single-particle subspace, which implies that the Hamiltonian H_0 is single-particle chiral symmetric: for a given single-particle eigenstate $|\epsilon_k\rangle$ of eigenenergy ϵ_k , $\hat{P} |\epsilon_k\rangle$ is also an eigenstate of opposite energy $-\epsilon_k$.

The Hamiltonian H_0 can thus be formally diagonalized as $H_0 = \sum_{0 < k \leq L/2} \epsilon_k \gamma_k^\dagger \gamma_k - \epsilon_k \tilde{\gamma}_k^\dagger \tilde{\gamma}_k$ with a new set of fermionic operators $\gamma_k, \tilde{\gamma}_k$ defined as

$$\gamma_k^\dagger = \sum_i V_{ki} c_i^\dagger, \quad \tilde{\gamma}_k^\dagger = \sum_i (-1)^i V_{ki} c_i^\dagger, \quad (4)$$

where the matrix \mathbf{V} diagonalizes the coupling matrix \mathbf{A} . This enables the expansion of the operator \hat{P} in the eigenbasis as $\hat{P} = \sum_{0 < k \leq L/2} \hat{P}_k$ where $\hat{P}_k = \gamma_k^\dagger \tilde{\gamma}_k + \tilde{\gamma}_k^\dagger \gamma_k$, which exchanges the excitation in each k -subspace as $\hat{P}_k \gamma_k^\dagger |0\rangle = \tilde{\gamma}_k^\dagger |0\rangle$. Properties of the operator \hat{P} will be further discussed in the Supplementary Material (SM) [38].

The key point is that for our choice of \hat{P} as the driving term, the chiral disordered model reduces to a collection of two level systems, *e.g.*, by introducing the ‘pseudospin’ representation $|\uparrow\rangle_k = \gamma_k^\dagger |0\rangle, |\downarrow\rangle_k = \tilde{\gamma}_k^\dagger |0\rangle$, the drive operator \hat{P}_k acts as the σ_x^k operator in each k -subspace. According to Eq. 4, the paired excitations have the same spatial wavefunction up to the $(-1)^i$ phase between neighboring sites. Consequently, the coupling between the paired states via \hat{P}_k will not significantly change the localization properties of the time evolution operator $U(t) = \mathcal{T} \left\{ \exp \left(-i \int_0^t dt' H(t') \right) \right\}$ in the single-particle subspace at any time t for arbitrary forms of the driving profile $f(t)$.

Crucially, this symmetry argument applies only to the single-particle subspace, but not to the multi-particle subspace, in which Eq. 3 generally does not vanish due to the presence of the operator \hat{D} . Although the spectrum for multiple particles remains symmetric, the operator \hat{P} does not simply map between multi-particle paired eigenstates of H_0 , but instead couples many (see SM). Nevertheless, the coupling is highly constrained as the total number of excitations in each k -subspace, $N_k = \gamma_k^\dagger \gamma_k + \tilde{\gamma}_k^\dagger \tilde{\gamma}_k$, is a conserved quantity! It trivially commutes with the Hamiltonian H_0 , but it crucially also commutes with \hat{P} which can only convert the excitation at a fixed k but cannot mix different k subspaces [38]. The extensive number of conserved quantities N_k , which are local because of the localized single-particle spectrum of H_0 , can

protect many-particle states from delocalization.

This conservation law can be broken by single-particle chiral symmetry-breaking perturbations, *e.g.*, static on-site disorder $\sum_i h_i n_i$ with h_i randomly chosen from $[0, h_{max}]$. It mixes different k -subspaces, hence, eigenstates of the time evolution operator $U(t)$ may become delocalized. However, as we will illustrate in the following, if $f(t)$ is periodic or constant, additional potential disorder will not delocalize the system but rather enhance the localization. Delocalization only happens when $f(t)$ is aperiodic, hence, highlighting the great importance of the conservation law in protecting the localization especially when TTS is absent.

Numerical results.— Although when N_k is conserved, the concrete form of the driving profile $f(t)$ is irrelevant for the persistent localization, here we choose for concreteness the discrete quasi-periodic Thue-Morse (TM) sequence which enables us to probe exponentially long times [20, 26, 27]. By defining two Hamiltonians

$$H_{\pm} = H_0 + \sum_i h_i n_i \pm \delta h \hat{P}, \quad (5)$$

one can construct two unitary evolution operators $U_{\pm} = \exp(-iT H_{\pm})$, with the characteristic time scale T . One can recursively define the following unitary operators

$$U_{n+1} = \tilde{U}_n U_n, \quad \tilde{U}_{n+1} = U_n \tilde{U}_n, \quad (6)$$

with $U_1 = U_- U_+$ and $\tilde{U}_1 = U_+ U_-$. The unitary time evolution for TM drive at stroboscopic times $t_m = 2^m T$ is obtained as $|\psi(t_m)\rangle = U_m |\psi(0)\rangle$ [27]. For Floquet systems, to diagnose the localization properties of single-particle eigenstates, one can use the participation ratio (PR) defined as $R_k = 1/\sum_i |\psi_i^k|^4$, where ψ_i^k denotes the k -th eigenfunction at site i of the Floquet operator [39, 40]. To quantify the average spreading of the eigenvectors in real space, the average PR is defined over all eigenstates and different disorder realizations $\bar{R} = \langle R_k \rangle_{k,r}$. For general delocalized states, one obtains $\bar{R}/L \sim O(1)$, whereas for perfectly localized ones $\bar{R}/L \sim 1/L$ [40]. However, in contrast to Floquet systems, a time-independent Floquet time evolution operator and its eigenstates are not available for our aperiodic system. Alternatively, $\bar{R}(t)/L$ is computed via the instantaneous eigenstates of the time evolution operator U_m at each stroboscopic time $t = 2^m T$.

As shown in Fig. 1 (a), for the case without potential disorder $h_{max} = 0$, the average PR \bar{R}/L remains at a constant small value indicating that single-particle eigenstates of the evolution operator remain localized. Indeed, for each

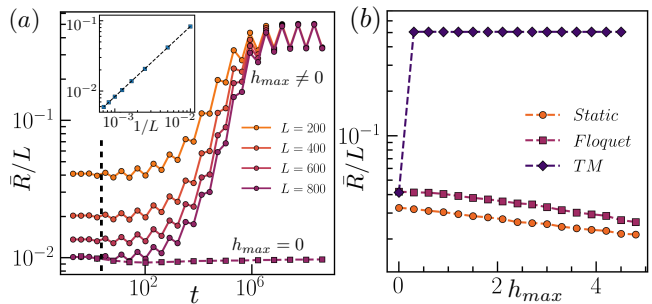


FIG. 1. (a) Average PR for eigenstates of the single-particle time evolution operator U_m at time $t = 2^m T$. Results are calculated for different system sizes and averaged over 100 disorder realization. The PR remains low in the absence of potential disorder, whereas a finite value $h_{max} = 0.51$ results in delocalization. The inset shows the size dependence of \bar{R}/L at $t \approx 10$ and the scaling $1/L$ is obtained to confirm the localization for short time. (b) PR for the static Hamiltonian, Floquet operator and TM driving after sufficiently long time $t \approx 10^{12}$ computed for $L = 200$. Potential disorder leads to stronger localization in static and Floquet systems, while any non-vanishing h_{max} delocalizes the system driven quasi-periodically. We use $J_0 = 1, J_{max} = 1.6\pi, \delta h = 1, h_{max} = 0.51, 1/T = 10$ for the simulation.

k -subspace, in the long-time limit, the time evolution operator recursively determined by Eq. 6 can be directly diagonalized by $|\uparrow\rangle_k$ and $|\downarrow\rangle_k$, the same eigenstates of the static Hamiltonian H_0 [20, 38]. In contrast, the inclusion of potential disorder drastically changes the behavior as different k -subspaces start to mix: following a plateau at low values for finite time $t \sim 10^2$, \bar{R}/L rapidly grows to system size independent values ($O(1)$) indicating delocalization. We verified that delocalization occurs for any nonzero value h_{max} as shown in Fig. 1 (b) where the average PR at a long time $t \approx 10^{12}$ is plotted. As a comparison, for the Floquet operator $U_- U_+$ and the static Hamiltonian H_+ , the average \bar{R}/L always reduces for larger h_{max} suggesting that eigenstates are more localized. Such a comparison suggests that the single-particle chiral symmetry protection becomes particularly crucial for aperiodic drives.

To verify the existence of persistent localization in multi-particle systems and to quantify the delocalization crossover at late times in the presence of a potential disorder, we next study the entanglement entropy $S_L(t) = -\text{Tr}[\rho_{L/2} \log_2 \rho_{L/2}]$ with the reduced density matrix $\rho_{L/2}$ of the half chain.

The initial state is chosen as a random product state with zero entanglement in the total magnetization $S_z = 0$ sector (or half-filling in the fermionic representation). After switching on the drive, the system starts generating entanglement and

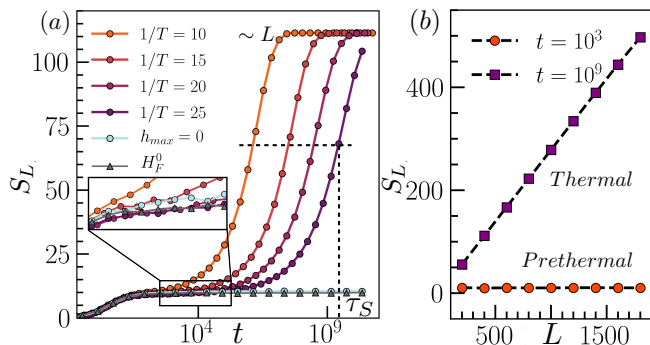


FIG. 2. (a) Entanglement dynamics for different driving rates, with or without potential disorder, averaged over 100 disorder realization and different initial states. Steady state can be delocalized by a non-vanishing potential disorder and thermalize. (b) System size dependence of the entanglement entropy. Prethermal (red dots) and the final plateau (purple squares) exhibit an area- and volume-law scaling respectively. We use parameters $J_0 = 1$, $J_{max} = 1.6\pi$, $\delta h = 1$, $h_{max} = 0.51$, $L = 400$ for the simulation.

its dynamics for varying driving rates $1/T$ is plotted in Fig. 2 (a). In the absence of the potential disorder (blue), as eigenstates of U_m always remain localized, entanglement can only be generated within limited regions. Therefore, it saturates around $t \approx 10^2$ at a low value after a transient process, suggesting the appearance of a persistent localized steady state protected by the conservation law of N_k . Once we turn on the potential disorder, localization becomes prethermal with a finite but long lifetime τ_S for large driving rates, e.g. $1/T \geq 15$. This prethermal localization can be well captured by an effective Hamiltonian (gray triangles), $H_{\text{eff}}^0 = (H_+ + H_-)/2$, obtained from the average of the two driving Hamiltonians [26].

As illustrated in the inset, the prethermal plateau (gray triangles) is slightly below the result for the steady state (blue), implying that the additional potential disorder leads to enhanced prethermal localization despite the fact that it eventually delocalizes the system at late times.

The entanglement entropy exhibits a well-pronounced increase after the time scale τ_S towards the final plateau, suggesting the eventual delocalization. As illustrated in Fig. 2 (b), in contrast to the prethermal entanglement which is system size independent (orange dots), the final plateau exhibits volume-law scaling (purple squares) demonstrating that entanglement has been established extensively over the whole system. However, as the system is non-interacting, it does not heat up to infinite temperature. The final entanglement entropy is smaller than the average entropy for a random state, i.e., the Page value $S_\infty = (L \log 2 - 1)/2$ [41].

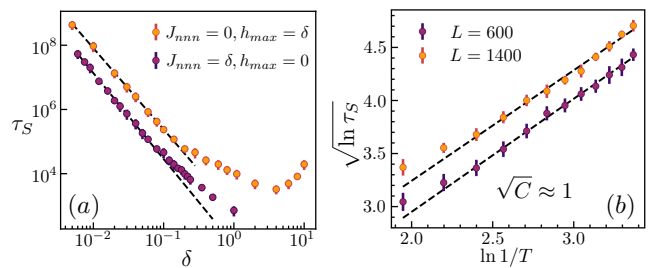


FIG. 3. (a) Algebraic dependence of τ_S on chiral symmetry-breaking perturbation δ with parameter $1/T = 1$, $L = 1400$. Dashed black lines correspond to the algebraic fit $\delta^{-2.6}$. (b) Delocalization time $\sqrt{\ln \tau_S}$ versus driving rate $\ln 1/T$ with parameter $h_{max} = 1.1$, $J_{nnn} = 0$. The numerical data fits well with a straight line of slope $\sqrt{C} \approx 1$, indicating τ_S behaves like $\tau_S \sim e^{C[\ln(T^{-1}/g)]^2}$. Both figures use $J_0 = 1$, $J_{max} = 1.6\pi$, $\delta h = 1$ and 100 disorder average.

Prethermal lifetime.— For weak breaking of the conservation law delocalization only occurs after a sufficiently long time scale. In Fig. 3 (a), we show the dependence of the delocalization time τ_S on different single-particle chiral symmetry-breaking perturbations of strength δ . To quantify the dependence, one can extract the time t_x at which the entanglement entropy crosses the threshold $S_L(t_x)/(L/2) = x$. The prethermal lifetime τ_S is then defined as the average $\tau_S = \langle t_x \rangle_x$ where the averaged is performed by using five different thresholds $x = s_0 \pm \epsilon$, $s_0 \pm \epsilon/2$, s_0 with the parameter values $s_0 = 0.11$ and $\epsilon = 0.02$.

It is worth noting that the driving frequency ($1/T = 1$) is comparable to other energy scales of H_0 . Hence, the prethermal localization cannot be predicted via a local effective Hamiltonian obtained from a high-frequency perturbative expansion [27]. However, the prethermal localization can still be parametrically long-lived as it is protected by approximately conserved quantities N_k . In the case of the small potential disorder $h_{max} = \delta$ (orange circles), the data fits well with a straight line in the log-log scale, suggesting that τ_S decreases algebraically as $\tau_S \propto \delta^{-\beta}$ with $\beta \approx 2.6$. Interestingly, for $\delta > 0.2$, a clear deviation from the scaling is observed and a turning point appears around $\delta \approx 5$, after which the prethermal lifetime instead increases monotonically. This suggests that beyond this point, instead of playing the role of a symmetry breaking perturbation, potential disorder stabilizes the localization and prolongs the prethermal lifetime.

Similarly, single-particle chiral symmetry can also be broken by introducing a static next-nearest-neighbor hopping $J_{nnn}/2 \sum_i (c_i^\dagger c_{i+2} + c_{i+2}^\dagger c_i)$ to H_0 and approximately the

same scaling exponent β is extracted (purple circles). However, in contrast to potential disorder, long-range hopping cannot stabilize the localization, hence no turning point exists.

The prethermal lifetime τ_S also increases with the driving rate $1/T$, and we extract τ_S similar to above, but with $s_0 = 0.13$, $\epsilon = 0.01$. We plot $\sqrt{\ln \tau_S}$ versus $\ln 1/T$ in Fig. 3 (b) for two system sizes with nonzero potential disorder h_{max} . The numerical results fit well with a straight line of slope $\sqrt{C} \approx 1$ in the high frequency regime, indicating that the prethermal lifetime scales as $\tau_S \sim e^{C[\ln(T^{-1}/g)]^2}$ with a local energy scale g as proposed in Ref. [27]. This scaling grows faster than any power law in $1/T$ but slower than exponential [27, 38].

Conclusion and Discussion.— We have identified a persistent localized steady state in a quasi-periodically driven multi-particle non-interacting system. The single-particle chiral symmetry and the resulting conservation law for multi-particle states account for this behavior. One can also add higher powers of the drive operator \hat{P} to the Hamiltonian, which leads to a long-range interaction and precludes the solvability of the model. However, as shown in the SM [38], such interaction cannot delocalize the system as it preserves the conservation law.

An analogous idea can be readily applied to systems hosting quantum many-body scars [42, 43] generated from, for instance, Hilbert space fragmentation [44–47] or a spectrum generating algebra [48–50]. As long as the fragmented structure is preserved by the drive, or the spectrum generating local ‘ladder’ operator [51], which only couples low-entangled scared states, is modulated aperiodically, the system eventually will not thermalize.

The additional potential disorder, which breaks the single-particle chiral symmetry, spoils the conservation law and the system delocalizes after a long prethermal localized regime. Although the dependence of the prethermal lifetime on the driving frequency is well-understood for the TM drive, a microscopic description of the delocalization process and its dependence on the symmetry breaking is still missing and worth exploring in the future. In a related vein, a framework for the description of localization in the absence of a natural time-independent time evolution operator – or perhaps a theory of the long-time convergence of the time evolution operators of aperiodic sequences – would be highly desirable.

Acknowledgements.— We acknowledge helpful discussion with Simon Lieu and Andrea Pizzi. We acknowledge support from the Imperial-TUM flagship partnership. HZ ac-

knowledges support from a Doctoral-Program Fellowship of the German Academic Exchange Service (DAAD). This work was partly supported by the Deutsche Forschungsgemeinschaft under grants SFB 1143 (project-id 247310070) and the cluster of excellence ct.qmat (EXC 2147, project-id 390858490).

-
- [1] Achilleas Lazarides, Arnab Das, and Roderich Moessner. Equilibrium states of generic quantum systems subject to periodic driving. *Phys. Rev. E*, 90(1):012110, July 2014.
 - [2] Dmitry A Abanin, Wojciech De Roeck, and François Huveneers. Exponentially slow heating in periodically driven many-body systems. *Physical review letters*, 115(25):256803, 2015.
 - [3] Tomotaka Kuwahara, Takashi Mori, and Keiji Saito. Floquet–magnus theory and generic transient dynamics in periodically driven many-body quantum systems. *Annals of Physics*, 367:96–124, 2016.
 - [4] Achilleas Lazarides, Arnab Das, and Roderich Moessner. Periodic thermodynamics of isolated quantum systems. *Phys. Rev. Lett.*, 112:150401, Apr 2014.
 - [5] Dmitry A Abanin and Zlatko Papić. Recent progress in many-body localization. *Annalen der Physik*, 529(7):1700169, 2017.
 - [6] Achilleas Lazarides, Arnab Das, and Roderich Moessner. Fate of many-body localization under periodic driving. *Physical review letters*, 115(3):030402, 2015.
 - [7] Pedro Ponte, Z. Papić, François Huveneers, and Dmitry A. Abanin. Many-Body Localization in Periodically Driven Systems. *Phys. Rev. Lett.*, 114(14):140401, April 2015.
 - [8] Vedika Khemani, Achilleas Lazarides, Roderich Moessner, and S. L. Sondhi. Phase structure of driven quantum systems. *Phys. Rev. Lett.*, 116:250401, Jun 2016.
 - [9] Dominic V. Else, Bela Bauer, and Chetan Nayak. Floquet time crystals. *Phys. Rev. Lett.*, 117:090402, Aug 2016.
 - [10] Paraj Titum, Erez Berg, Mark S Rudner, Gil Refael, and Natan H Lindner. Anomalous floquet-anderson insulator as a nonadiabatic quantized charge pump. *Physical Review X*, 6(2):021013, 2016.
 - [11] Albert Verdeny, Joaquim Puig, and Florian Mintert. Quasi-periodically driven quantum systems. *Zeitschrift für Naturforschung A*, 71:897–907, July 2016.
 - [12] Philipp T Dumitrescu, Romain Vasseur, and Andrew C Potter. Logarithmically slow relaxation in quasiperiodically driven random spin chains. *Physical review letters*, 120(7):070602, 2018.
 - [13] Dominic V Else, Wen Wei Ho, and Philipp T Dumitrescu. Long-lived interacting phases of matter protected by multiple time-translation symmetries in quasiperiodically driven systems. *Physical Review X*, 10(2):021032, 2020.
 - [14] David M Long, Philip JD Crowley, and Anushya Chandran. Many-body localization with quasiperiodic driving. *arXiv*

- preprint *arXiv:2108.04834*, 2021.
- [15] Ivar Martin, Gil Refael, and Bertrand Halperin. Topological frequency conversion in strongly driven quantum systems. *Physical Review X*, 7(4):041008, 2017.
- [16] Philip JD Crowley, Ivar Martin, and Anushya Chandran. Topological classification of quasiperiodically driven quantum systems. *Physical Review B*, 99(6):064306, 2019.
- [17] Simon Körber, Lorenzo Privitera, Jan Carl Budich, and Björn Trauzettel. Interacting topological frequency converter. *Physical Review Research*, 2(2):022023, 2020.
- [18] Eric Boyers, Philip J. D. Crowley, Anushya Chandran, and Alexander O. Sushkov. Exploring 2d synthetic quantum hall physics with a quasi-periodically driven qubit, 2020.
- [19] Hongzheng Zhao, Florian Mintert, and Johannes Knolle. Floquet time spirals and stable discrete-time quasicrystals in quasiperiodically driven quantum many-body systems. *Phys. Rev. B*, 100:134302, Oct 2019.
- [20] Sourav Nandy, Arnab Sen, and Diptiman Sen. Aperiodically driven integrable systems and their emergent steady states. *Physical Review X*, 7(3):031034, 2017.
- [21] Bastien Lapiere, Kenny Choo, Apoorv Tiwari, Clément Tauber, Titus Neupert, and Ramasubramanian Chitra. Fine structure of heating in a quasiperiodically driven critical quantum system. *Physical Review Research*, 2(3):033461, 2020.
- [22] Xueda Wen, Ruihua Fan, Ashvin Vishwanath, and Yingfei Gu. Periodically, quasiperiodically, and randomly driven conformal field theories. *Physical Review Research*, 3(2):023044, 2021.
- [23] David M Long, Philip JD Crowley, and Anushya Chandran. Nonadiabatic topological energy pumps with quasiperiodic driving. *Physical Review Letters*, 126(10):106805, 2021.
- [24] Frederik Nathan, Rongchun Ge, Snir Gazit, Mark Rudner, and Michael Kolodrubetz. Quasiperiodic floquet-thouless energy pump. *Physical Review Letters*, 127(16):166804, 2021.
- [25] Zihao Qi, Gil Refael, and Yang Peng. Universal nonadiabatic energy pumping in a quasiperiodically driven extended system. *arXiv preprint arXiv:2110.07757*, 2021.
- [26] Hongzheng Zhao, Florian Mintert, Roderich Moessner, and Johannes Knolle. Random multipolar driving: tunably slow heating through spectral engineering. *Physical Review Letters*, 126(4):040601, 2021.
- [27] Takashi Mori, Hongzheng Zhao, Florian Mintert, Johannes Knolle, and Roderich Moessner. Rigorous bounds on the heating rate in thue-morse quasiperiodically and randomly driven quantum many-body systems. *Physical Review Letters*, 127(5):050602, 2021.
- [28] Romain Vasseur, Aaron J Friedman, SA Parameswaran, and Andrew C Potter. Particle-hole symmetry, many-body localization, and topological edge modes. *Physical Review B*, 93(13):134207, 2016.
- [29] Giuseppe De Tomasi, Daniele Trapin, Markus Heyl, and Soumya Bera. Anomalous diffusion in particle-hole symmetric many-body localized systems. *arXiv preprint arXiv:2001.04996*, 2020.
- [30] Daniel S Fisher. Random antiferromagnetic quantum spin chains. *Physical review b*, 50(6):3799, 1994.
- [31] Freeman J. Dyson. The dynamics of a disordered linear chain. *Phys. Rev.*, 92:1331–1338, Dec 1953.
- [32] C. M. Soukoulis and E. N. Economou. Off-diagonal disorder in one-dimensional systems. *Phys. Rev. B*, 24:5698–5702, Nov 1981.
- [33] L Fleishman and DC Licciardello. Fluctuations and localization in one dimension. *Journal of Physics C: Solid State Physics*, 10(6):L125, 1977.
- [34] Giuseppe De Tomasi, Sthitadhi Roy, and Soumya Bera. Generalized dyson model: Nature of the zero mode and its implication in dynamics. *Physical Review B*, 94(14):144202, 2016.
- [35] Michael A Nielsen. The fermionic canonical commutation relations and the jordan-wigner transform. *School of Physical Sciences The University of Queensland*, 2005.
- [36] János K Asbóth, László Oroszlány, and András Pályi. The suschrieffer-heeger (ssh) model. In *A Short Course on Topological Insulators*, pages 1–22. Springer, 2016.
- [37] Shinsei Ryu, Andreas P Schnyder, Akira Furusaki, and Andreas WW Ludwig. Topological insulators and superconductors: tenfold way and dimensional hierarchy. *New Journal of Physics*, 12(6):065010, 2010.
- [38] Details regarding the chiral symmetry, localization in the long-time limit, comparison between different fitting methods and effects of additional interactions are discussed in the supplementary material.
- [39] Sthitadhi Roy, Ivan Khaymovich, Arnab Das, and Roderich Moessner. Multifractality without fine-tuning in a floquet quasiperiodic chain. *SciPost Phys*, 4(025):032117–12, 2018.
- [40] Bernhard Kramer and Angus MacKinnon. Localization: theory and experiment. *Reports on Progress in Physics*, 56(12):1469, 1993.
- [41] Don N Page. Average entropy of a subsystem. *Physical review letters*, 71(9):1291, 1993.
- [42] Christopher J Turner, Alexios A Michailidis, Dmitry A Abanin, Maksym Serbyn, and Zlatko Papić. Weak ergodicity breaking from quantum many-body scars. *Nature Physics*, 14(7):745–749, 2018.
- [43] Maksym Serbyn, Dmitry A Abanin, and Zlatko Papić. Quantum many-body scars and weak breaking of ergodicity. *Nature Physics*, 17(6):675–685, 2021.
- [44] Pablo Sala, Tibor Rakovszky, Ruben Verresen, Michael Knap, and Frank Pollmann. Ergodicity breaking arising from hilbert space fragmentation in dipole-conserving hamiltonians. *Physical Review X*, 10(1):011047, 2020.
- [45] Vedika Khemani, Michael Hermele, and Rahul Nandkishore. Localization from hilbert space shattering: From theory to physical realizations. *Physical Review B*, 101(17):174204, 2020.
- [46] Ana Hudomal, Ivana Vasić, Nicolas Regnault, and Zlatko Papić. Quantum scars of bosons with correlated hopping. *Communications Physics*, 3(1):1–12, 2020.

- [47] Hongzheng Zhao, Joseph Vovrosh, Florian Mintert, and Johannes Knolle. Quantum many-body scars in optical lattices. *Physical review letters*, 124(16):160604, 2020.
- [48] Sanjay Moudgalya, Nicolas Regnault, and B Andrei Bernevig. Entanglement of exact excited states of affleck-kennedy-lieb-tasaki models: Exact results, many-body scars, and violation of the strong eigenstate thermalization hypothesis. *Physical Review B*, 98(23):235156, 2018.
- [49] Michael Schecter and Thomas Iadecola. Weak ergodicity breaking and quantum many-body scars in spin-1 x y magnets. *Physical review letters*, 123(14):147201, 2019.
- [50] Naoto Shiraishi and Takashi Mori. Systematic construction of counterexamples to the eigenstate thermalization hypothesis. *Physical review letters*, 119(3):030601, 2017.
- [51] Nicholas O’Dea, Fiona Burnell, Anushya Chandran, and Vedika Khemani. From tunnels to towers: Quantum scars from lie algebras and q-deformed lie algebras. *Physical Review Research*, 2(4):043305, 2020.

THE CHIRAL SYMMETRY

Here discuss details of the chiral symmetry. In the literature [28, 29], instead of using the single-particle chiral symmetry generator \hat{P} , chiral symmetry for a fermionic system with Hamiltonian $H_C = \sum_{ij} c_i^\dagger A_{ij} c_j$ is defined via the generator $\mathcal{S} = \mathcal{R} \times \mathcal{T}$, where \mathcal{R} represents the particle-hole transformation $\mathcal{R} c_i^\dagger \mathcal{R}^{-1} = (-1)^i c_i$ and time reversal $\mathcal{T} c_i^\dagger \mathcal{T} = c_i^\dagger, \mathcal{T} i \mathcal{T}^{-1} = -i$. The time reversal symmetry ensures that the matrix \mathbf{A} is real and the particle-hole transformation takes the Hamiltonian to

$$\begin{aligned} \mathcal{R} H_C \mathcal{R}^{-1} &= \sum_{ij} (-1)^i c_i A_{ij} c_j^\dagger (-1)^j \\ &= \sum_{ij} (-1)^{i+j+1} c_j^\dagger A_{ij} c_i + \text{tr}(\mathbf{A}) \\ &= \sum_{i \neq j} (-1)^{i+j+1} c_i^\dagger A_{ij} c_j - \sum_i A_{ii} n_i + \text{tr}(\mathbf{A}). \end{aligned} \quad (7)$$

As the initial Hamiltonian reads

$$H_C = \sum_{i \neq j} c_i^\dagger A_{ij} c_j + \sum_i A_{ii} n_i, \quad (8)$$

by comparing it with Eq. 7, we know that to preserve the chiral symmetry, the off-diagonal term needs to satisfy the condition

$$(-1)^{i+j+1} A_{ij} = A_{ij}, \quad (9)$$

and any diagonal terms in \mathbf{A} has to be zero. Eq. 9 suggests that if $A_{ij} \neq 0$, $(-1)^{i+j+1}$ has to be 1, leading to the conclusion that $i+j$ is odd; otherwise, A_{ij} is zero. These conditions guarantee that $\mathcal{S} H_C \mathcal{S}^{-1} = H_C$. Therefore, if $|\epsilon_\alpha\rangle$ is an eigenstate

of H_C with eigenenergy ϵ_α , $\mathcal{S} |\epsilon_\alpha\rangle$ is also an eigenstate with the same eigenenergy. However, these two eigenstates might not have the same particle number as the particle-hole transformation does not conserve it.

For a single-particle state, Eq. 9 naturally leads to the anti-commutation relation $\{H_C, \hat{P}\} = 0$ as $(-1)^i + (-1)^j$ in Eq. 3 has to be zero. The Hamiltonian H_0 defined below Eq. 2 in the main content is one special case with only nearest-neighbor hopping. \hat{P} is unitary in the single-particle subspace with the property

$$\hat{P}^2 = \mathcal{I}, \quad (10)$$

where \mathcal{I} denotes the identity. The vanishing anti-commutator also implies that for a given single-particle eigenstate $|\epsilon_k\rangle$ of eigenenergy ϵ_k , $\hat{P} |\epsilon_k\rangle$ is another eigenstate of energy $-\epsilon_k$. Such a property sharply distinguishes the effect of \mathcal{S} and \hat{P} .

In the multi-particle subspace, Eq. 10 is not true. Also, the anti-commutator $\{H_C, \hat{P}\} = \hat{D}$, with $\hat{D} = 2 \sum_{ijk} (-1)^k A_{ij} c_i^\dagger n_k c_j$, is generally non-vanishing for a multi-particle state. For example, consider a single body Fock state $|\phi\rangle_1 = c_p^\dagger |0\rangle$, we then have

$$\hat{D} |\phi\rangle_1 = \sum_{ij} A_{ij} c_i^\dagger \delta_{jp} \left(\sum_k (-1)^k n_k \right) |0\rangle, \quad (11)$$

where the number operator yields zero. However, for a two-body Fock state $|\phi\rangle_2 = c_p^\dagger c_q^\dagger |0\rangle$, one can verify that

$$\hat{D} |\phi\rangle_2 = \sum_i A_{ip} (-1)^q c_i^\dagger c_q^\dagger |0\rangle \quad (12)$$

$$- \sum_i A_{iq} (-1)^p c_i^\dagger c_p^\dagger |0\rangle, \quad (13)$$

which is a non-zero superposition of two-body Fock states. Therefore, $\{H_C, \hat{P}\} = 0$ is valid only in the single particle subspace. For this reason we call \hat{P} the ‘single-particle chiral symmetry generator’ to distinguish it from the more standard chiral symmetry operator \mathcal{S} .

REPRESENTATION OF \hat{P} IN THE EIGENBASIS

Here we will show how to expand $\hat{P} = \sum_i (-1)^i n_i$ in the eigenbasis. By using the transformation

$$c_i = \sum_{0 < k \leq L/2} V_{ki} \gamma_k + \sum_{0 < k \leq L/2} (-1)^i V_{ki} \tilde{\gamma}_k,$$

we obtain

$$\hat{P} = \sum_i (-1)^i \left(\sum_{0 < q \leq L/2} V_{qi}^* \gamma_q^\dagger + \sum_{0 < q \leq L/2} (-1)^i V_{qi}^* \tilde{\gamma}_q^\dagger \right) \times \left(\sum_{0 < k \leq L/2} V_{ki} \gamma_k + \sum_{0 < k \leq L/2} (-1)^i V_{ki} \tilde{\gamma}_k \right), \quad (14)$$

where four combinations appear if we expand the product. However, two of them yield zero, for instance

$$\begin{aligned} & \sum_i (-1)^i \sum_{0 < q \leq L/2} V_{qi}^* \gamma_q^\dagger \sum_{0 < k \leq L/2} V_{ki} \gamma_k \\ &= \sum_{0 < q, k \leq L/2} \gamma_q^\dagger \gamma_k \sum_i (-1)^i V_{ki} [V^\dagger]_{iq} \\ &= \sum_{0 < q, k \leq L/2} \gamma_q^\dagger \gamma_k \sum_i V_{\bar{k}i} [V^\dagger]_{iq} \end{aligned} \quad (15)$$

where we define $V_{\bar{k}i} = (-1)^i V_{ki}$. Suppose V_{ki} represents the k -th eigenstate of energy ϵ_k , then $V_{\bar{k}i}$ corresponds to its paired state of energy $-\epsilon_k$. We also know $\sum_i V_{\bar{k}i} [V^\dagger]_{iq} = \delta_{\bar{k}, q}$, which turns to be zero because $L/2 < \bar{k} \leq L$ whereas $0 < q \leq L/2$. Therefore, Eq. 15 gives zero. On the contrary, the following term is nonzero:

$$\begin{aligned} & \sum_i (-1)^i \sum_{0 < q \leq L/2} V_{qi}^* \gamma_q^\dagger \sum_{0 < k \leq L/2} V_{ki} \tilde{\gamma}_k (-1)^i \\ &= \sum_{0 < q, k \leq L/2} \gamma_q^\dagger \tilde{\gamma}_k \sum_i V_{ki} [V^\dagger]_{iq} \\ &= \sum_{0 < q, k \leq L/2} \gamma_q^\dagger \tilde{\gamma}_k \delta_{k, q} = \sum_{0 < k \leq L/2} \gamma_k^\dagger \tilde{\gamma}_k. \end{aligned} \quad (16)$$

In the end, we obtain $\hat{P}_k = \gamma_k^\dagger \tilde{\gamma}_k + \tilde{\gamma}_k^\dagger \gamma_k$.

EFFECT OF \hat{P} ON DIFFERENT EIGENSTATES

As we discussed in the main content, \hat{P} couples the paired single-particle excitations of opposite energy. However, this will not be the case if we consider a multi-particle system. For example, we can consider the ground state $|\lambda_{GS}\rangle = \prod_{0 < j < L/2} \tilde{\gamma}_j^\dagger |0\rangle$ where all negative energies are occupied. Operator \hat{P} excites each of them forming a superposition as

$$\hat{P} |\lambda_{GS}\rangle = \sum_{0 < i < L/2} (-1)^{L/2-i} \prod_{0 < j < L/2, j \neq i} \tilde{\gamma}_j^\dagger \gamma_i^\dagger |0\rangle, \quad (17)$$

where the phase factor comes from anti-commutation relation for fermions. This state is different from the state $\prod_{0 < j < L/2} \gamma_j^\dagger |0\rangle$ of energy $\sum_{0 < j < L/2} \epsilon_j$ as the symmetric counterpart of the ground state at the top edge of the multi-particle spectrum. In addition, Eq. 17 indicates that the

ground state is only coupled with $L/2$ excited states of energy $-\sum_{0 < j < L/2} \epsilon_j + 2\epsilon_i$, which is only a small fraction of the whole spectrum. Repeated application of \hat{P} will couple more excitations. However, excitations at the same absolute energy cannot be simultaneously populated as the total occupation number N_k for each k must be conserved.

Another interesting two-body eigenstate is the one occupying both excitations at the same absolute energy:

$$|\lambda_k\rangle = \gamma_k^\dagger \tilde{\gamma}_k^\dagger |0\rangle. \quad (18)$$

This eigenstate has zero energy and does not couple to any other eigenstates via the operator \hat{P} because $\hat{P}_k |\lambda_k\rangle = 0$ holds.

COMMUTATION BETWEEN N_k AND P_k

Here we show that the total number of excitations excitation $N_k = \gamma_k^\dagger \gamma_k + \tilde{\gamma}_k^\dagger \tilde{\gamma}_k$ at a fixed k commutes with the drive $\hat{P} = \sum_{0 < k \leq L/2} \gamma_k^\dagger \tilde{\gamma}_k + \tilde{\gamma}_k^\dagger \gamma_k$. As terms in different k -subspaces commute, we only need to check whether the following commutator $[P_k, \gamma_k^\dagger \gamma_k + \tilde{\gamma}_k^\dagger \tilde{\gamma}_k]$ vanishes. It involves two contributions and the first one reads

$$\begin{aligned} [P_k, \gamma_k^\dagger \gamma_k] &= [\gamma_k^\dagger \tilde{\gamma}_k + \tilde{\gamma}_k^\dagger \gamma_k, \gamma_k^\dagger \gamma_k] \\ &= [\gamma_k^\dagger \tilde{\gamma}_k, \gamma_k^\dagger \gamma_k] + [\tilde{\gamma}_k^\dagger \gamma_k, \gamma_k^\dagger \gamma_k] \\ &= \gamma_k^\dagger \tilde{\gamma}_k \gamma_k^\dagger \gamma_k - \gamma_k^\dagger \gamma_k \tilde{\gamma}_k^\dagger \gamma_k + [\tilde{\gamma}_k^\dagger \gamma_k, \gamma_k^\dagger \gamma_k] \\ &= 0 - \gamma_k^\dagger (1 - \gamma_k^\dagger \gamma_k) \tilde{\gamma}_k + [\tilde{\gamma}_k^\dagger \gamma_k, \gamma_k^\dagger \gamma_k] \\ &= -\gamma_k^\dagger \tilde{\gamma}_k + [\tilde{\gamma}_k^\dagger \gamma_k, \gamma_k^\dagger \gamma_k], \end{aligned} \quad (19)$$

where we use $(\gamma_k^\dagger)^2 = 0$. In the end we get

$$[P_k, \gamma_k^\dagger \gamma_k] = -\gamma_k^\dagger \tilde{\gamma}_k + \tilde{\gamma}_k^\dagger \gamma_k. \quad (20)$$

The second contribution can be obtained similarly as $[P_k, \tilde{\gamma}_k^\dagger \tilde{\gamma}_k] = -\tilde{\gamma}_k^\dagger \gamma_k + \gamma_k^\dagger \tilde{\gamma}_k$. It cancels Eq.20, hence we obtain $[P_k, \gamma_k^\dagger \gamma_k + \tilde{\gamma}_k^\dagger \tilde{\gamma}_k] = 0$.

LOCALIZATION IN THE LONG-TIME LIMIT

Using a pseudo-spin representation, one can rewrite the elementary time evolution operator for each subspace labeled by k in the form

$$U_{\pm}^k = \exp[-iT E_k (\sin \gamma_k \sigma_z^k \pm \cos \gamma_k \sigma_x^k)], \quad (21)$$

with $E_k = \sqrt{\epsilon_k^2 + \delta h^2}$, and $\sin \gamma_k = \epsilon_k / E_k$, $\cos \gamma_k = \delta h / E_k$. The unitary operator recursively determined by Eq. 6 converges to $U_{\infty}^k = \exp(-i\alpha_{\infty}^k \sigma_z)$ in the limit $n \rightarrow \infty$ with

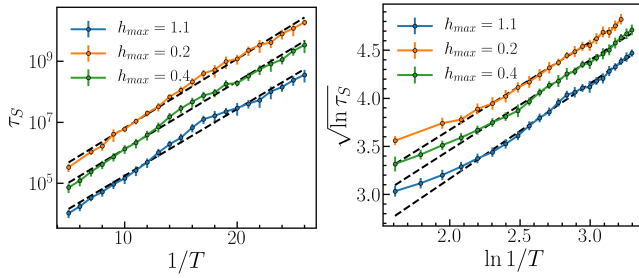


FIG. 4. $J_0 = 1, J_{max} = 1.6\pi, \delta h = 1, L = 600$.

a nonsaturating phase factor α_n^k [20]. Hence, in the asymptotic limit it is diagonal in the z direction, and U_∞^k can directly be diagonalized by $|\uparrow\rangle_k, |\downarrow\rangle_k$, the same eigenstates of the static Hamiltonian H_0 .

COMPARISON BETWEEN DIFFERENT FITS

Here we extract the delocalization time by averaging the time t such that $S_L(t)/(L/2) = 0.2 \pm 0.04, 0.2, 0.2 \pm 0.02$, and compare different fitting methods. In the left panel of Fig. 4, we plot the numerical data in the log scale and fit it with the exponential scaling

$$\tau_S \sim \exp(\alpha T^{-1}). \quad (22)$$

The slope of the linear fit corresponds to the scaling exponent $\alpha \approx 0.5$. The numerical data curve deviates from a straight dashed line, suggesting that the heating time is shorter than exponential. As a comparison, in the right panel we perform the fitting only for $1/T > 7$, and the data fit well with

$$\tau_S \sim e^{C[\ln(T^{-1}/g)]^2}, \quad (23)$$

with $\sqrt{C} \approx 1$. Both the scaling parameters \sqrt{C} and α do not depend on h_{max} .

INTERACTION EFFECTS

As shown in Fig. 2 of the main text, the final entanglement plateau does not reach the Page value. It indicates that although the system thermalizes, the final state is not the infinite temperature state because the system is non-interacting. Here we introduce the interaction in z direction as a perturbation to

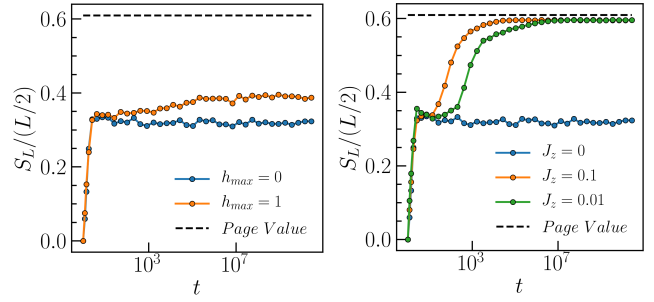


FIG. 5. $J_0 = 1, J_{max} = 1.6\pi, \delta h = 1, T^{-1} = 10$.

explicitly break the integrability. The Hamiltonian then reads

$$H_\pm = H_0 + \frac{1}{2} \sum_{i=1}^L h_i^\pm \sigma_i^z, \quad (24)$$

$$H_0 = \frac{1}{4} \sum_{i=1}^{L-1} J_i (\sigma_i^x \sigma_{i+1}^x + \sigma_i^y \sigma_{i+1}^y) + J_z \sigma_i^z \sigma_{i+1}^z,$$

and the simulation is performed via exact diagonalization for system size $L = 12$. The result is plotted in Fig. 5.

First, let us focus on the non-interacting case (blue data in the left panel) with $J_z = 0$ and $h_{max} = 0$ where the entanglement quickly saturates after a transient relaxation. However, we notice this value still depends on system size indicating that the simulation is limited by the finite size effect. Nonzero h_{max} (orange dots) delocalizes the system and entanglement increases and saturates at a value smaller than the Page value $S_L = (L \log 2 - 1)/2$ (black dashed line) corresponding to the infinite temperature state.

In contrast, as shown in the right panel, even for $h_{max} = 0$, the interaction $J_z \sum_i \sigma_i^z \sigma_{i+1}^z$ delocalizes the system. This happens because $J_z \sum_i \sigma_i^z \sigma_{i+1}^z$ breaks the conservation law N_k , even though it is invariant under the chiral transformation S up to a constant. As this perturbation also breaks the integrability, the final saturation is close to the Page value, suggesting eventual thermalization to infinite temperature.

Alternatively, we also consider interactions which preserve the conservation of N_k , for instance \hat{P}^2 . In terms of spin operators, up to a constant, this term can be expressed as

$$H_s = \frac{J_s}{4} \sum_{i,j} (-1)^{i+j} \sigma_i^z \sigma_j^z, \quad (25)$$

which is an infinitely long-range interaction in z direction. The full driving now reads

$$H_\pm = H_0 + \frac{1}{2} \sum_{i=1}^L h_i^\pm \sigma_i^z \pm H_s. \quad (26)$$

As shown in Fig. 6 left panel, starting from the domain-wall initial state $|\uparrow \dots \uparrow \downarrow \dots \downarrow\rangle$ with zero total magnetization, the system maintains the memory of the initial state for small values of J_s , suggesting that the system is localized in the presence of the conservation-preserving interaction. However, as shown in the right panel, non-vanishing J_s tends to generate more entanglement than the non-interacting case. The steady state does not heat up to infinite temperature because the system is localized and N_k is conserved.

The comparison between different types of interactions highlights that the persistent localization is protected by the single-particle chiral symmetry generated by \hat{P} , instead of the chiral symmetry generated by \mathcal{S} .

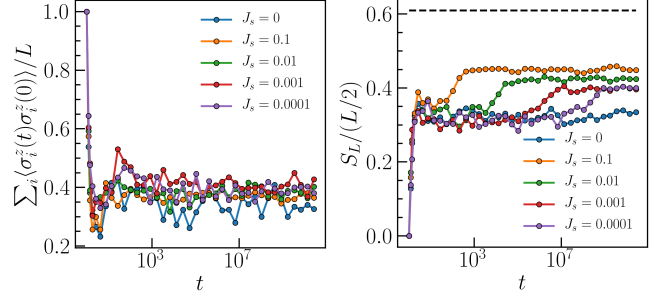


FIG. 6. $J_0 = 1, J_{max} = 20, \delta h = 1, h_{max} = 0, 1/T = 10$.